Density hardening plasticity and mechanical ageing of silica glass under pressure: a Raman spectroscopic study

2008 J. Phys.: Condens. Matter 20 485221

(http://iopscience.iop.org/0953-8984/20/48/485221)

IOP Publishing Journal of Physics: Condensed Matter

J. Phys.: Condens. Matter **20** (2008) 485221 (6pp) doi:10.1088/0953-8984/20/48/485221

Density hardening plasticity and mechanical ageing of silica glass under pressure: a Raman spectroscopic study

Damien Vandembroucq[1,2], Thierry Deschamps[3], Camille Coussa[3], Antoine Perriot[2], Etienne Barthel[2], Bernard Champagnon[3] and Christine Martinet[3]

[1] Laboratoire de Physique et Mécanique des Milieux Hétérogènes, PMMH UMR 7636 CNRS/ESPCI/Paris 6/Paris 7, 10 rue Vauquelin, F-75231 Paris cedex 05, France
[2] Laboratoire Surface du Verre et Interfaces, Unité Mixte de Recherche CNRS/Saint-Gobain, 39 Quai Lucien Lefranc, F-93303 Aubervilliers, France
[3] Université de Lyon; Université Lyon1; UMR5620 CNRS Laboratoire de Physico-Chimie des Matériaux Luminescents, Domaine Scientifique de la Doua, Bâtiment Kastler, 10 rue Ampère, Villeurbanne, F-69622, France

E-mail: damienvdb@pmmh.espci.fr

Received 9 May 2008, in final form 19 September 2008
Published 28 October 2008
Online at stacks.iop.org/JPhysCM/20/485221

Abstract
In addition to a flow, plastic deformation of structural glasses (in particular amorphous silica) is characterized by a permanent densification. Raman spectroscopic estimators are shown to give a full account of the plastic behavior of silica under pressure. While the permanent densification of silica has been widely discussed in terms of amorphous–amorphous transition, from a plasticity point of view, the evolution of the residual densification with the maximum pressure of a pressure cycle can be discussed as a density hardening phenomenon. In the framework of such a mechanical ageing effect, we propose that the glass structure could be labeled with the maximum pressure experienced by the glass and that the saturation of densification could be associated with the densest packing of tetrahedra only linked by their vertices.

(Some figures in this article are in colour only in the electronic version)

1. Introduction

The behavior of amorphous silica under high pressure has been intensively studied in the last few decades [1–7] and has recently motivated an increasing amount of numerical studies [8–17]. Silica appears to be elastic up to around 10 GPa and to exhibit a plastic behavior at higher pressure. Two features can be emphasized at that level: (i) in the elastic regime, the compressibility exhibits a surprising non-monotonic evolution with a maximum at around 2–3 GPa [1, 18, 19], (ii) when unloading from the plastic regime a permanent densification up to 20% can be observed [1–7]. No clear evidence of alteration of the tetrahedral short-range order in this unloaded state has been observed [5, 20].

Above 25 GPa, a change from fourfold to sixfold coordination is observed [5]. This sixfold amorphous seems not to be quenchable at zero pressure. When unloading down to zero pressure, no trace of sixfold coordination is obtained. Performing x-ray Raman scattering experiments on the oxygen K edge, Lin *et al* [21] observed a reversible electronic bonding transition between 10 and 25 GPa. The latter was attributed to a fourfold quartz-like to a sixfold stishovite-like change of configuration of silica glass. For $P > 25$ GPa the densification process saturates and, after unloading to ambient, the density level is the one obtained with a maximum pressure $P \simeq 25$ GPa [18, 19].

Questions remain about the nature of the densified phase and the mechanism of densification. Recent studies [17] have proposed the existence of an 'activated' fivefold coordination at high pressure allowing reorganization toward a denser tetrahedral network. In former studies, by analogy with amorphous ice, Lacks [12] has proposed a first-order transition

between two different tetrahedral amorphous phases of silica. This transition would be kinetically hindered at room temperature. This idea of polyamorphism has received a lot of attention [7, 14–16, 22–26]. At this stage it is important to separate the known transition at very HP between a fourfold amorphous silica and a sixfold amorphous silica involving a change in the short-range order [5, 9] from an additional hypothetical transition at lower P between two different amorphous phases of tetrahedral silica and involving the medium-range order [27].

The most recent numerical [17] and experimental [7] works as well as the existence of a continuous range of densities for amorphous silica [6] after the return to ambient pressure seem to rule out this idea of a transition between two different forms of amorphous tetrahedral silica. However, the original observation of Lacks remains of interest: performing molecular dynamics simulations driven by volume [11], he noted discontinuities in the pressure signal associated with local pressure induced mechanical instabilities. The latter are reminiscent of the shear induced mechanical instabilities previously identified in flowing liquids [28]. Note that similar localized transitions are widely believed to be the main mechanism of shear plasticity of amorphous materials [29] and can be associated with the vanishing of one eigenvalue of the Hessian matrix of the interatomic potential [30, 31].

In parallel with a structural study, it may be worth considering the pressure induced densification process in silica according to a mechanical perspective. In particular, in the Raman spectroscopic measurements to be presented below, we will use cycles of pressure of increasing maxima. This protocol will help us to discriminate in the spectral patterns modifications due to the reversible elastic deformation of the network from other ones due to plastic structural reorganizations.

We first present the experimental methods, i.e. Raman measurements of silica subjected to pressure cycles, and analyze the results in terms of mechanical behavior. Two series of experiments are discussed. In series **A** Raman measurements are performed *in situ* during the loading and unloading stages of successive pressure cycles. In series **B** Raman measurements are performed *ex situ* at ambient pressure before and after pressure cycles of increasing maximum pressure.

The results of these spectroscopic measurements are presented in the next section and discussed in the framework of continuum plasticity. The first series of *in situ* experiments gives a nice illustration of (densification) plasticity in the context of a silica glass while the second series of experiments allows us to follow the evolution of permanent densification versus the pressure maximum of the cycle, i.e. the density hardening behavior of silica.

We finally give a discussion, first in terms of mechanical behavior, then in terms of amorphous structure. These results are of primary importance in the description of the mechanical properties of silica. While silica is in daily use as a calibration sample for nanoindentation measurements, it appears that the mechanical behavior of this material is not fully described. It has been shown recently [32] that the constitutive laws available [33, 34] which do not take hardening into account fail to fully describe the densification process induced by an indentation test. The above data can be used to include hardening in a simple constitutive law of silica [35], which gives a precise account for this behavior.

Beyond their interest in terms of mechanical behavior, these results can also be discussed in terms of amorphous structure. In particular, as detailed below, densification can be regarded as a typical glassy phenomenon, resulting from a mechanical ageing process. Following this perspective, the amorphous densified structure would be associated with the quench of the structure at high pressure and could be labeled with a fictive pressure in the very same way as a fictive temperature can be used to label a structure obtained by thermal ageing.

2. Experimental methods

Bars of amorphous silica (Saint-Gobain Quartz IDD) are shattered into pieces. Splinters of characteristic length of 10 μm are subjected to cycles of pressure in a 'Sidoine'[4] diamond-anvil cell (DAC) with a maximum pressure in the range 1–25 GPa. Raman spectra are collected with a Renishaw RM 1000 microspectrometer (with a Ar^+-ion 514 nm, 50 mW laser excitation). A small piece of ruby is introduced together with the silica splinter in order to monitor the pressure level using the shift of the R1 luminescence band.

Two series of experiments are presented.

- In series **A** *in situ* measurements of the Raman spectrum are collected throughout the compression cycle. Three cycles are presented, The first one with $P_{max} = 7.3$ GPa lies in the elastic domain, and the second cycle consists of a compression up to $P_{max} = 18$ GPa followed by a decompression at 1 GPa; finally the last cycle consists of a compression up to $P_{max} = 16$ GPa and a direct return to ambient pressure induced by the breakdown of a diamond. Methanol is used as a pressure transmitting fluid in this series of experiments (quasi-hydrostatic conditions). A detailed presentation of these *in situ* experiments can be found in [36].
- In series **B** Raman measurements are performed *ex situ* at ambient pressure before and after each cycle of pressure. A series of compression cycles is presented where the pressure maximum is increasing from 9 GPa for the first cycle to 25 GPa for the last cycle. In this case, the pressure transmitting fluid is a mix similar to 5:1 methanol–ethanol, which ensures hydrostaticity up to 16–20 GPa [37]. The Raman spectrum is measured before loading and after unloading, the diamond-anvil cell being emptied of the transmitting fluid.

Figure 1 contrasts the initial spectrum of a sample (plain line) and that obtained after a 18 GPa hydrostatic loading (dotted line).

Between 200 and 750 cm^{-1} we can identify a main band at 440 cm^{-1}. This band is intense, and affected by the densification process: the band gets narrower and is

[4] Institut de Minéralogie et de Physique des Milieux Condensés (Paris).

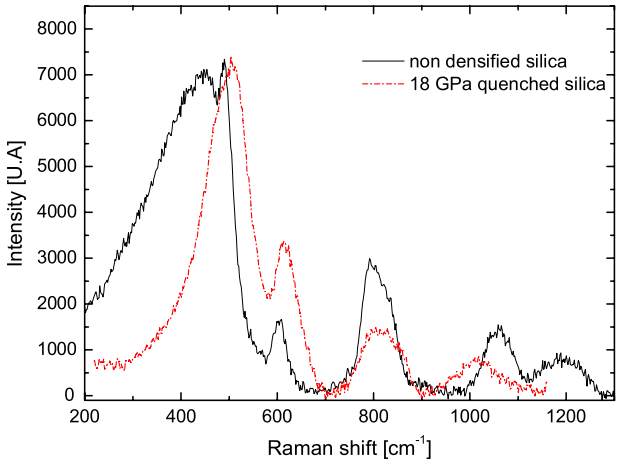

Figure 1. Raman spectra obtained with an amorphous silica sample before (plain line) and after (dotted line) a 18 GPa hydrostatic loading.

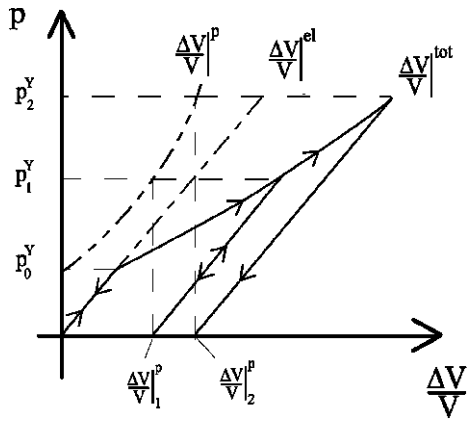

Figure 2. Sketch of a typical pressure/density curve expected in elasto-plasticity. A reversible elastic behavior is obtained up to the elastic limit pressure P_0^Y. When loading above P_0^Y, plasticity sets in and the (elastic) unloading from P_1^Y is characterized by a residual densification. A subsequent loading at $P_2^Y > P_1^Y$ reproduces the previous unloading curve up to P_1^Y before plasticity sets in again. The elastic limit has thus evolved under loading from P_0^Y to P_1^Y and P_2^Y. The knowledge of this density hardening behavior (evolution of the limit elastic pressure with density at zero pressure) is necessary to give a proper modeling of the plasticity of glasses.

shifted to higher wavenumbers. This band was originally attributed to the symmetric stretching mode of bridging oxygens between two Si atoms and its evolution under densification to the decrease of the inter-tetrahedral angles Si–O–Si [38]. Recent determinations of the Raman spectrum from first principles [39] have established that this broad band originates more probably from bending motions of oxygen atoms that do not belong to small rings.

The defect lines D_1 and D_2, at 492 and 605 cm^{-1}, are respectively attributed to the breathing modes of the four-membered and three-membered rings [13, 40, 41]. Their area ratio was previously used in the literature as an indicator for the variation of the 'fictive temperature' [42–44], which is associated with a slight change of density. The effect of pressure seems to be better accounted for by the shift of the D_2 line. As discussed by Polsky *et al* [45], this may be due to pressure induced variations of the Raman cross section. The D_2 line is of particular interest since it has almost no overlap with the main band. Sugiura *et al* [46] correlated the position of the D_2 line with the ratio of the sample density ρ to its initial density ρ_0. The residual density evaluated through this relation accounts for both irreversible and elastic densifications due to residual elastic strain. However, several works [46–48] evidenced that the D_2 line position is only marginally sensitive to residual elastic strains. This correlation was recently used to probe the densification gradient surrounding a plastic imprint in silica obtained by indentation [32].

3. Results and interpretation

We describe in the following the experimental results and give an interpretation in the framework of the elasto-plastic response of continuous media.

3.1. Continuum mechanics

We first recall briefly the formalism of elasto-plasticity. Figure 2 shows the hydrostatic stress as a function of the volumetric strain for a medium subjected to pressure. Below a threshold value of pressure P_0^Y the material remains fully elastic and the volumetric deformation is reversible. On increasing the pressure beyond threshold, plasticity sets in and an irreversible deformation adds up to the elastic reversible deformation. When unloading from $P_1^Y > P_0^Y$, the material behaves elastically and only the elastic part of deformation is recovered. Loading again to a higher pressure $P_2^Y > P_1^Y$, we observe the same phenomenology with a crucial difference: the onset of plasticity has increased from P_0^Y to P_1^Y. In other words, the mechanical behavior depends on the history of the mechanical loading. The material has experienced hardening [49] which can be regarded as a mechanical ageing. Such a behavior is standard for metal shear plasticity and usually results at the structural level from the entanglement or the pinning of dislocations by impurities [50]. Metals however do not exhibit any volumetric plastic deformation (dislocation motion is a volume conserving mechanism). However, irreversible changes of density are familiar in soil mechanics and granular materials (dilatancy effect) [51].

The typical mechanical behavior of a material like silica glass can be summarized as follows. Before any loading, the material is elastic up to a threshold which depends both on pressure and shear. Using hydrostatic pressure p and equivalent shear stress τ as coordinates, this elastic threshold corresponds to a continuous curve intersecting the two axes. On reaching the threshold, if the stress is increased, plasticity sets in and the elastic limit is moved to the maximum value of stress experienced by the material. At the macroscopic scale, one tries to characterize this hardening behavior, relating the evolution of densification to the pressure maximum. At the microscopic scale, in the present case of silica, in the absence of a microscopic mechanism as well defined as the motion of

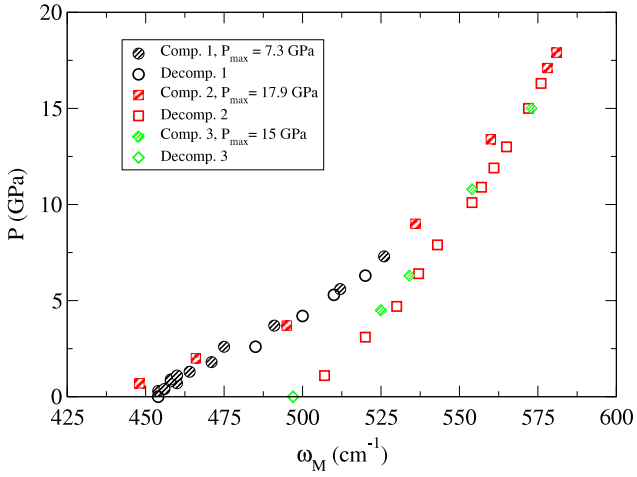

Figure 3. Raman shift of the main band ω_M in the elastic–plastic regime. Successive pressure loading and unloading cycles are depicted. Filled and empty symbols correspond to loading and unloading curves, respectively. For a pressure maximum $P_{max} = 7.3$ GPa, a full reversibility is obtained (elastic behavior). For a larger maximum pressure $P_{max} = 18$ GPa, a residual shift is obtained after unloading (plastic behavior). An additional loading at $P_{max} = 16$ GPa reproduces the last unloading curve, indicating the increase of the elastic limit under loading (hardening).

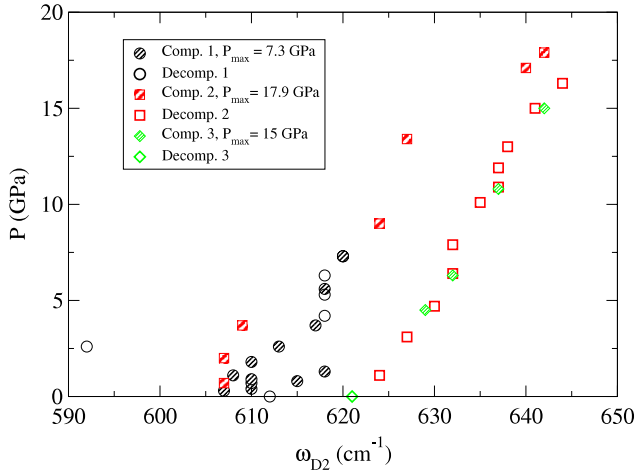

Figure 4. Raman shift of the D_2 line ω_{D_2} in the elastic–plastic regime (the same conditions as figure 3).

the dislocation, the question of identifying and understanding a structural signature of density hardening remains.

3.2. Elasto-plastic behavior of silica under pressure

In this section we present the results of *in situ* Raman measurements (series **A**). Two patterns of the Raman spectra measured *in situ* during the pressure cycles are discussed: (i) the shift of the main band ω_M; (ii) the shift of the D_2 line ω_{D_2}.

In figures 3 and 4 we show the evolution of the positions of these two bands for a cycle of pressure up to $P_{max} = 7.3$ GPa (black symbols). We observe a full reversibility between loading and unloading. This result is consistent with the usual estimate $P_c \simeq 10$ GPa for the onset of permanent densification in silica. The evolution of these indicators is also plotted in the same figures for the second series of cycles up to $P_{max} = 17.9$ GPa. We now see that below $P_c \simeq 10$ GPa, the same elastic behavior as before is recovered; then a change of slope on loading is noticeable at least for the position of the main band; then the unloading curve does not reproduce the initial loading one and there appears a permanent change of the spectrum at ambient pressure; on loading again, one follows the very last unloading curve. These two curves appear to be very similar to the ideal case of hardening plasticity depicted in figure 2. This spectroscopic study allows us to closely follow the elastic–plastic behavior of silica under pressure.

We now discuss the evolution of permanent densification after cycles of increasing pressure. Even if the signal-to-noise ratio is less favorable for the determination of the D_2 line than for the main band (see figure 3 versus figure 4), we choose the former for estimating the permanent densification. As discussed above, the main reason for this choice is that in contrast to the case for the main band, the shift of the D_2 line appears to be rather independent of the elastic stress. This allows us to use it a density probe for samples affected by residual elastic stress. Because of the microscopic size of the silica samples used in the diamond-anvil cell, a quantitative calibration could not be performed. Densification can be obtained for millimetric samples but this requires high temperature treatments [6] and it is far from obvious that the medium-range order is directly comparable to the one obtained under high pressure at ambient temperature. Following [32], the densification was estimated using the empirical relation

$$\frac{\Delta\omega_{D_2}}{\omega_{D_2}} \simeq \left(\frac{\Delta\rho}{\rho}\right)^{0.14}, \qquad (1)$$

which was extracted from the experimental data of Sugiura *et al* [46] obtained in shock wave experiments. This calibration step is thus only approximative.

The results are summarized in figure 5. We thus obtain the evolution of the permanent densification with the pressure maximum P^Y of each pressure cycle. We obtain a continuous range of increasing densities with an apparent saturation. As shown in figure 5, this evolution can be approached by a sigmoidal curve. Comparable results were obtained recently on window glass using an octahedral multi-anvil apparatus [52]. In mechanical terms, this allows us to give a quantitative account of the density hardening behavior of silica. In the space of stresses, we have obtained the evolution of the maximum pressure P^Y below which the material remains fully elastic as a function of the glass density.

4. Discussion

Raman spectroscopic estimators have been shown to give a full account of the density hardening behavior of silica under pressure. Raman scattering measurements during a loading/unloading pressure cycle closely reproduce the elasto-plastic behavior usually observed in stress/strain curves: full reversibility below a limit stress, appearance of a residual

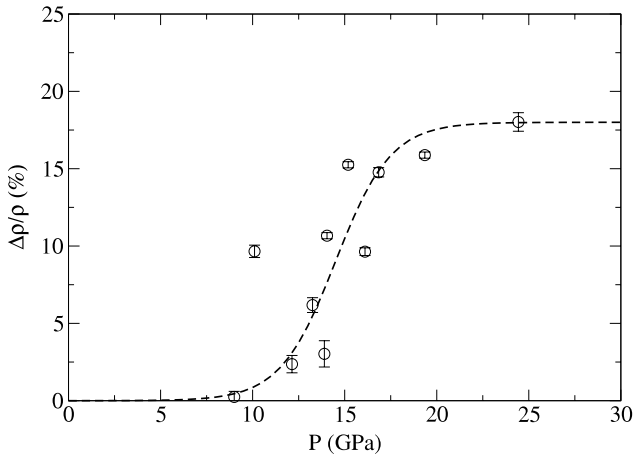

Figure 5. Evolution of the residual densification versus the maximum pressure of the pressure cycle (symbols). The dashed line is an indicative sigmoidal curve corresponding to 18% of maximum densification.

deformation with an elastic unloading for larger stresses. A crucial difference obviously lies in the fact that in the present study the evolution of hydrostatic pressure versus density is considered instead of shear stress versus shear strain as in usual metal plasticity. From a mechanical point of view, the detailed analysis of the density increase with the maximum pressure of the cycle allowed us to study the evolution of the residual densification with the elastic limit pressure P^{Y}. Such knowledge is of crucial importance for the determination of the constitutive equation modeling the plastic behavior of silica. It was shown in [32] that when restricting the plastic criterion to perfect plasticity (i.e. assuming no hardening effect) it was not possible to account for the permanent densification of amorphous silica around a plastic imprint induced by indentation. Conversely, as shown in [35], the assumption of an elliptic plastic criterion coupling shear stress and pressure, together with the data for density hardening extracted from the present experiments, allows one to successfully describe this phenomenon of indentation induced densification.

From a physical/structural point of view, the present results suggest that the description of densified silica need not involve the hypothesis of an amorphous–amorphous transition between tetrahedral networks of two types. A simpler and alternative scenario consists of pressure induced reorganizations of the amorphous network allowing a more efficient packing of tetrahedra remaining linked by their vertices only. Such a scenario does not exclude the occurrence of fivefold-or sixfold-coordinated silica in the plastic regime at high pressure. However, the latter would correspond to intermediate states between two amorphous tetrahedral structures. This occurrence of fivefold or sixfold coordination would thus simply indicate the necessity of cutting and rebonding between the two structures. The denser structure would thus be quenched when pressure decreases down to ambient conditions. In that sense, the final structure could be labeled with the maximum pressure that the material experienced. In this context of mechanical ageing, the latter pressure could be thought of as a 'fictive' pressure in the same way as the fictive temperature in a more classical thermal ageing experiment. Note that these denser structures may be affected by internal stresses due to the succession of localized reorganizations. More generally, these results indicate that the structure and the density of a densified sample of vitreous silica will depend crucially on the particular path that it has followed in the plane pressure/temperature: it is likely that the medium-range structure of densified silica is not fully characterized by the only density parameter.

Looking finally at orders of magnitude for the density of the various phases of silica, we observe that the density of the stable crystalline equivalent at zero pressure (quartz) is 2.65 while the density of the metastable coesite (stable at 2–3 GPa) is 3.01. The density of fused silica being 2.2, a 20% increase gives 2.64, i.e. values close to quartz ones but well below coesite ones. Considering hexagonal and random close packing, an interesting question could thus be whether the maximum observed density of amorphous silica corresponds to any geometrical maximal packing of tetrahedra bonded by their vertices only, i.e. the maximum density of the continuous random network. To our knowledge, though the packing of space with tetrahedra or ellipsoids has been considered [53, 54], this question has not been discussed yet.

Acknowledgments

The authors acknowledge useful discussions with G Kermouche, W Kob and S Ispas-Crouzet. They would like to thank CECOMO and High Pressure Facilities of University Lyon1. This work was supported by the ANR 'plastiglass' contract ANR-05-BLAN-0367-01.

References

[1] Bridgman P W and Simon I 1953 *J. Appl. Phys.* **24** 405
[2] Cohen H M and Roy R 1961 *J. Am. Ceram. Soc.* **44** 523
[3] Mackenzie J D 1963 *J. Am. Ceram. Soc.* **46** 461
[4] Polian A and Grimsditch M 1990 *Phys. Rev.* B **41** 6086
[5] Meade C, Hemley R J and Mao H K 1992 *Phys. Rev. Lett.* **69** 1387
[6] Inamura Y, Arai M, Nakamura M, Otomo T, Kitamura N, Bennington S M, Hannon A C and Buchenau U 2001 *J. Non-Cryst. Solids* **293–295** 389
[7] Inamura Y, Katayama Y, Utsumi W and Funakoshi K I 2004 *Phys. Rev. Lett.* **93** 015501
[8] Jin W, Kalia R K, Vashishta P and Rino J P 1993 *Phys. Rev. Lett.* **71** 3146
[9] Jin W, Kalia R K, Vashishta P and Rino J P 1994 *Phys. Rev.* B **50** 118
[10] Valle R G D and Venuti E 1996 *Phys. Rev.* B **54** 3809
[11] Lacks D J 1998 *Phys. Rev. Lett.* **80** 5385
[12] Lacks D J 2000 *Phys. Rev. Lett.* **84** 4629
[13] Rahmani A, Benoit M and Benoit C 2003 *Phys. Rev.* B **68** 184202
[14] Dávila L P, Caturla M J, Kubota A, Sadigh B, de la Rubia T D, Shackelford J F, Risbud S H and Garofalini S H 2003 *Phys. Rev. Lett.* **91** 205501
[15] Huang L and Kieffer J 2004 *Phys. Rev.* B **69** 224203
[16] Huang L and Kieffer J 2004 *Phys. Rev.* B **69** 224204
[17] Liang Y, Miranda C R and Scandolo S 2007 *Phys. Rev.* B **75** 024205
[18] Polian A and Grimsditch M 1993 *Phys. Rev.* B **47** 13979

[19] Zha C S, Hemley R J, Mao H K, Duffy T S and Meade C 1994 *Phys. Rev.* B **50** 13105
[20] Hemley R J, Mao H K, Bell P M and Mysen B O 1986 *Phys. Rev.* B **57** 747
[21] Lin J-F *et al* 2007 *Phys. Rev.* B **75** 012201
[22] Saika-Voivod I, Sciortino F and Poole P H 2001 *Nature* **41** 514
[23] Mukherjee G D, Vaidya S N and Sugandhi V 2001 *Phys. Rev. Lett.* **87** 195501
[24] Shell M S, Debenedetti P G and Panagiotopoulos A Z 2002 *Phys. Rev.* E **66** 011202
[25] Saika-Voivod I, Sciortino F, Grande T and Poole P H 2004 *Phys. Rev.* E **70** 061507
[26] Champagnon B, Martinet C, Coussa C and Deschamps T 2007 *J. Non-Cryst. Solids* **353** 4208
[27] Poe B T, Romano C and Henderson G 2004 *J. Non-Cryst. Solids* **341** 162
[28] Malandro D L and Lacks D J 1998 *Phys. Rev. Lett.* **81** 5576
[29] Falk M L and Langer J S 1998 *Phys. Rev.* E **57** 7192
[30] Maloney C E and Lemaître A 2004 *Phys. Rev. Lett.* **93** 195501
[31] Maloney C E and Lemaître A 2006 *Phys. Rev.* E **74** 016118
[32] Perriot A, Martinez V, Martinet C, Champagnon B, Vandembroucq D and Barthel E 2006 *J. Am. Ceram. Soc.* **89** 596
[33] Shorey A, Xin K, Chen K and Lambropoulos J 1998 *Proc. SPIE* **3424** 72
[34] Xin K and Lambropoulos J 2000 *Proc. SPIE* **4102** 112
[35] Kermouche G, Barthel E, Vandembroucq D and Dubujet P 2008 *Acta Mater.* **56** 3222
[36] Champagnon B, Martinet C, Boudeulle M, Vouagner D, Coussa C, Deschamps T and Grosvalet L 2008 *J. Non-Cryst. Solids* **354** 569
[37] Besson J and Pinceaux P 1979 *Rev. Sci. Instrum.* **50** 541
[38] Mochizuki S and Kawai N 1972 *Solid State Commun.* **11** 763
[39] Umari P, Gonze X and Pasquarello A 2003 *Phys. Rev. Lett.* **90** 027401
[40] Galeneer F L 1982 *Solid State Commun.* **44** 1037
[41] Pasquarello A and Car R 1998 *Phys. Rev. Lett.* **80** 5145
[42] Champagnon B, Chemarin C, Duval E and Parc R L 2000 *J. Non-Cryst. Solids* **274** 81
[43] Parc R L, Champagnon B, Guenot P and Dubois S 2001 *J. Non-Cryst. Solids* **293–295** 367
[44] Champagnon B, Parc R L and Guenot P 2002 *Phil. Mag.* B **82** 251
[45] Polsky C H, Smith K H and Wolf G H 1999 *J. Non-Cryst. Solids* **248** 159
[46] Sugiura H, Ikeda R, Kondo K and Yamadaya T 1997 *J. Appl. Phys.* **81** 1651
[47] Hibino Y, Hanafusa H, Ema K and Hyodo S-I 1985 *Appl. Phys. Lett.* **47** 812
[48] Michalske T A, Tallant D and Smith W L 1988 *Phys. Chem. Glasses* **29** 150
[49] Khan A and Huang S 1995 *Continuum Theory of Plasticity* (New York: Wiley)
[50] Cottrell A H 1956 *Dislocations and Plastic Flow in Crystals* (Oxford: Oxford University Press)
[51] Jaeger H M, Nagel S and Behringer R P 1996 *Rev. Mod. Phys.* **68** 1259
[52] Ji H, Keryvin V, Rouxel T and Hammouda T 2006 *Scr. Mater.* **55** 1159
[53] Binder K and Kob W 2005 *Glassy Materials and Disordered Solids* (Singapore: World Scientific)
[54] Donev A, Stillinger F H, Chaikin P M and Torquato S 2004 *Phys. Rev. Lett.* **92** 255506